Preclinical Evidence of an Allogeneic Dual CD20xCD22 CAR to Target a Broad Spectrum of Patients with B-cell Malignancies

Beatriz Aranda-Orgilles[1], Isabelle Chion-Sotinel[2], Jordan Skinner[1], Steven Grudman[1], Ben Mumford[1], Chantel Dixon[1], Jorge Postigo Fernandez[1], Piril Erler[1], Phillipe Duchateau[2], Agnes Gouble[2], Roman Galetto[2], and Laurent Poirot[2]

ABSTRACT

Despite the remarkable success of autologous chimeric antigen receptor (CAR) T cells, some patients relapse due to tumor antigen escape and low or uneven antigen expression, among other mechanisms. Therapeutic options after relapse are limited, emphasizing the need to optimize current approaches. In addition, there is a need to develop allogeneic "off-the-shelf" therapies from healthy donors that are readily available at the time of treatment decision and can overcome limitations of current autologous approaches. To address both challenges simultaneously, we generated a CD20xCD22 dual allogeneic CAR T cell. Herein, we demonstrate that allogeneic CD20x22 CAR T cells display robust, sustained and dose-dependent activity *in vitro* and *in vivo*, while efficiently targeting primary B-cell non–Hodgkin lymphoma (B-NHL) samples with heterogeneous levels of CD22 and CD20. Altogether, we provide preclinical proof-of-concept data for an allogeneic dual CAR T cell to overcome current mechanisms of resistance to CAR T-cell therapies in B-NHL, while providing a potential alternative to CD19 targeting.

Introduction

With an estimated 544,000 new cases and 260,000 deaths reported worldwide in 2020 (1, 2), B-cell non–Hodgkin lymphoma (B-NHL) remains one of the most common cancers worldwide. Chimeric antigen receptor (CAR) T-cell therapies have brought enormous success to the treatment of B-cell malignancies, achieving high remission rates of up to 90% (3). Approved CAR T-cell therapies so far use autologous T cells engineered with a synthetic receptor to recognize a tumor-associated antigen. Despite the groundbreaking efficacy of current CAR T-cell therapies, studies on patients treated with autologous CAR T cells are revealing several causes for relapses including antigen loss, low antigen expression, and insufficient CAR T-cell potency and persistence, among others (4, 5). The limited number of eligible treatment options after CAR T-cell relapse and for patients not eligible for autologous CAR T-cell therapies, underscores the urgent need to develop novel therapies with the potential to improve patient outcomes (6–8).

Patient-specific CAR T-cell production entails a high variability between processes and failures associated with individualized manufacturing, both of which can delay treatment availability. T-cell biology also plays a key role, because high tumor burden, immunosuppressive responses of the tumor microenvironment or the impact of previous treatments can make patient-derived CAR T cells dysfunctional and compromise treatment success. Indeed, emerging preclinical data show that CAR T cells generated from healthy donors can display superior activity against lymphoma, leukemia, or multiple myeloma (9–11).

Allogeneic cell therapies hold the promise to overcome some of the challenges posed by autologous therapies (7, 12). Consequently, an increasing number of allogeneic CAR T-cell therapies have reached preclinical and early stages of clinical development during the last years. Importantly, early clinical studies with gene-edited CAR T cells are showing promising preliminary results for allogeneic therapies (13, 14). There is mounting evidence on the efficacy and safety of CAR T cells genetically modified to inactivate the T-cell receptor alpha constant gene (*TRAC*) and *CD52* gene using TALEN to simultaneously prevent GVHD and enhance host lymphocyte suppression and depletion. Using this technology, UCART19, which targets CD19, was the first allogeneic CAR T-cell therapy in clinical trials, and reports continue to show encouraging data that demonstrate the efficacy and safety with single and consolidation dosing for the treatment of relapsed/refractory lymphoma (15, 16). Similar promising data are being observed with CAR T cells carrying the *TRAC*/*CD52* knockout genetic scaffold targeting different targets such as CD22 or BCMA (17). Other approaches using alternative editing strategies are also undergoing clinical trials with encouraging results (18, 19). Although more long-term studies are needed to gain a deeper understanding of the durability and long-term efficacy of allogeneic CAR T-cell therapies, these early data underscore the potential feasibility in the clinic of these approaches.

While several suitable targets to treat B-cell malignancies have been identified, CD19 has been the focus of attention leading to a crowded space with limited therapeutic alternatives for CD19-low or CD19-negative relapses (Supplementary Fig. S1; ref. 6). Moreover, although the outcomes for patients with B-NHL have improved with CD19-directed CAR T-cell therapies, only about 30% to 40% of patients experience long-lasting remission (20). Therefore, there is a need to identify and continue developing CAR T cells against additional suitable targets (21) that can be used either as an alternative or after relapsing from CD19-directed therapies. To approach this need, we developed UCART20x22, an allogeneic dual CAR T cell targeting two validated antigens commonly expressed in B-cell malignancies, CD20

[1]Cellectis, Inc., New York, New York. [2]Cellectis, SA, Paris, France.

Corresponding Authors: Beatriz Aranda-Orgilles, Innovation, Cellectis, Inc, 430 East, 29th St, New York, NY 10016. Phone: 347-752-4044; E-mail: beatriz.aranda-orgilles@cellectis.com; and Laurent Poirot, laurent.poirot@cellectis.com

Cancer Immunol Res 2023;11:946–61

doi: 10.1158/2326-6066.CIR-22-0910

and CD22, and whose expression is preserved after CD19 CAR T-cell treatment (refs. 22, 23; Supplementary Fig. S1). This strategy was designed with the goal of addressing some of the challenges identified in current CAR T-cell therapies including: (i) antigen escape caused by a single target such as low antigen expression or heterogeneous antigen distribution on tumor B cells; (ii) offer a therapeutic opportunity to treat CD19-negative relapses; (iii) manufacturing roadblocks for patients with dysfunctional or reduced numbers of T cells; and (iv) length of time from treatment decision to infusion. The FDA recently cleared an Investigational New Drug Application (IND) to initiate a phase I/IIa clinical trial using UCART20x22 for patients with refractory/relapsed B-cell lymphoma.

Herein, we provide preclinical proof of concept demonstrating potent and sustained activity of different designs of allogeneic CD20xCD22 CAR *in vitro* and *in vivo* against various antigen combinations. We also demonstrate that CD20xCD22 CAR has specific cytolytic activity *in vivo* against a patient-derived xenograft model and *in vitro* against primary B-NHL cells expressing a variety of CD20 and CD22 antigen densities, and we present several antigen escape models *in vitro* and *in vivo* that underscore the benefit that this therapy could provide to overcome current challenges in the treatment of relapsed/refractory B-cell lymphoma.

Materials and Methods

Peripheral blood mononuclear cells

Cryopreserved human peripheral blood mononuclear cells (PBMC) were acquired from ALLCELLS (PB006F) and used in accordance with Cellectis IRB/IEC-approved protocols. PBMCs were cultured in OpTmizer media (A10485-01) containing IL2 (Miltenyi Biotec, 130-097-748), and human serum AB (HS; Seralab, GEM-100-318). Next day, T cells were activated using TransAct beads (Miltenyi Biotec, 130-111-160) and cultured in complete OpTmizer media (OpTmizer media supplemented with 5% human AB serum and 20 ng/mL of human IL2).

Human-edited CAR T-cell generation

Four days after PBMC thawing and activation, T cells were transduced with recombinant lentiviral vectors (rLV) at a multiplicity of infection (MOI) of 15 for CD20xCD22 CAR and 5 for single CD22 and CD20 CARs, in retronectin-coated (Takara Bio USA Inc, T100B 30 μg/mL in PBS for 1 hour in untreated plates) culture vessels. LentiBOOST (SIRION Biotech, SB-P-LV-101-12) at a concentration of 1:50 was added to transductions performed with CD20xCD22 CAR. Cells were transduced in serum-free OpTmizer media at a concentration of 1.6×10^6 cells/mL and diluted to 1×10^6 cells/mL after 2 hours and supplemented with 5% human serum and 20 ng/mL IL2 and cultured at 37°C in the presence of 5% CO_2.

Two days after transduction, TALEN mRNA electroporation was performed using the Cellectis' PulseAgile Electroporation System to disrupt the *TRAC* and *CD52* genes (sequences in Supplementary Table S1). A total of 5 million activated and rLV-transduced PBMCs were transfected in each transfection with a total of 2.5 μg for each arm of TALEN mRNA using PulseAgile technology on day 6 after thawing (sequences in Supplementary Table S1). For transfection, cells were concentrated at 28×10^6 cells/mL in Cytoporation buffer T (BTX Harvard Apparatus). A total of 5×10^6 cells in 200 μL of BTX solution were transfected by applying two 0.1 ms pulses at 2,000 V/cm followed by four 0.2 ms pulses at 325 V/cm in 0.4 cm gap cuvettes. Electroporated cells were transferred to a 12-well plate containing 1 mL of prewarmed OpTmizer media (supplemented with human serum and IL2) and incubated at 37°C for 15 minutes. After transfection, cells were placed at 37°C for 15 minutes and transferred to 30°C overnight. Next day, cells were seeded at a density of 10^6 cells/mL in complete OpTmizer media with 5% HS and 20 ng/mL IL2 and cultivated at 37°C in the presence of 5% CO_2.

Cells were further cultured in complete OpTmizer media with 5% HS and 20 ng/mL IL2 and 2 days after transfection were transferred into 10 cm G-Rex or 6-well G-Rex devices (Wilson Wolf P/N 80240M or P/N 800405) using 35 mL of media. On day 11, IL2 at 20 ng/mL was added. On day 13, media was exchanged (OpTmizer media with 5% HS and 20 ng/mL IL2) and supplemented with 5% of Gibco CTS Immune Cell SR (Gibco #A4702901). Cells were grown until day 15 or day 18, when they were collected and frozen at 50 to 100 million cells/mL in FBS/10% DMSO.

Construction of lentiviral vectors

CARs directed against CD20 and CD22 were constructed by joining the respective single-chain variable fragments (scFV; refs. 24, 25) with the CD8α hinge/transmembrane domain (NP_001139345.1), 4-1BB (NP_001552.2), and CD3ζ (NP_932170.1) intracellular domains (Supplementary Table S1). All codon optimization and gene synthesis were performed by Genscript. The same CAR sequences were used for single CAR and dual CAR constructs, where they are separated by a P2A ribosome skip peptide derived from porcine teschovirus. Coding sequences were cloned downstream of the EF1a promoter and upstream of the wood chuck hepatitis virus posttranscriptional regulatory element (WPRE).

Lentivirus production, concentration, titration, and quantification

Viral particles were produced at Flash Therapeutics at small scale, and at research and development (R&D) grade. Briefly, viral-derived vectors were produced by tri-transfection into 293T cells by using standard transfection methods. A total of 24 hours later, cells were washed with fresh medium. Viral supernatants were collected and filtered through 0.45 μm filters and subjected to ultrafiltration for purification and concentration of virus particles. Titers were estimated by qPCR 72 hours after transduction of HCT116 cells by serial dilution of viral supernatants. A GFP expression lentiviral vector was used as control in each plate of titration.

Cell lines

Raji (ATCC #CCL-86; RRID:CVCL_0511, received in 2014), Daudi (ATCC # CCL-213; RRID:CVCL_0008, received in 2011), JeKo1 (ATCC# CRL-3006 cells, RRID: CVCL_1865, received in 2013), and MOLM-13 (DSMZ #ACC 554 RRID: CVCL_2119, received in 2014) were cultured in RPMI1640 (ATCC- 30-2001) with 10% (15% for MOLM-13) heat-inactivated FBS (Life Technologies, #16000-044), and 1% penicillin/streptomycin (Life Technologies, #15140-122). For heat inactivation, FBS was incubated at 56°C for 30 minutes and shaken every 20 minutes before being aliquoted and frozen. Cells were kept at a concentration of 0.5×10^6–1×10^6 cells/mL by passaging them every 2 to 3 days. For cell line authentication, banks of cells were prepared shortly after thawing original vials and cell morphology was monitored continuously under the microscope. Number of passages was limited to 7 to 10. The MycoAlert *Mycoplasma* Detection Kit from Lonza was used for *Mycoplasma* detection.

Daudi and JeKo1 reporter cell lines were generated by transducing the cells with a lentivirus encoding EF1a-Luciferase-2A-GFP (Neo; Amsbio #LVP438). The Raji-luc cell line was generated by transducing Raji cells with a lentivirus encoding Luciferase (firefly)-2A-GFP from

(Amsbio #LVP323). The Raji-Nanoluc cell line was generated by transducing a vector expressing nanoluc-2A-GFP, generated at Genescript and virus produced at Flash Therapeutics as indicated before (sequence provided in Supplementary Table S1)

Raji CD20- and CD22-negative cell lines were obtained upon electroporation of Raji-luc or Raji-nanoluc cell line with TALEN specific for *CD20* and *CD22* and subsequent purification of CD20-, CD22-, and double-negative populations with a SH800S Cell Sorter after labeling the cells for 30 minutes for CD20 and CD22 (see Supplementary Table S2 for antibodies). Briefly, Raji cells were washed with in Cytoporation buffer T and resuspended at 20×10^6 cells per mL, 100 μL cells were mixed with 0.8 μg of *CD20* TALEN (each arm) and 4 μg of *CD22* TALEN (each arm). Cells were then electroporated using PulseAgile technology at by applying two 0.1 ms pulses at 2,000 V/cm followed by four 0.2 ms pulses at 325 V/cm in 0.2 cm gap cuvettes. Sequences for both *CD20* and *CD22* TALEN are provided in Supplementary Table S1.

Qifikit assay

Quantification of CD20 and CD22 molecules in tumor cell lines was performed using the QIFIKIT assay from agilent (K0078) following the manufacturer's instructions. Briefly, 0.3×10^6 cells were washed with PBS-0.1% BSA buffer and after that resuspended in 100 μL buffer with 10 μL of antibody (CD20 or CD22, references indicated in Supplementary Table S2). Samples were stained for 30 minutes at 4°C and then washed with buffed by centrifugation at 1,500 rpm for 5 minutes). Afterward, the secondary antibody was added (Goat anti-mouse FITC, provided in kit) as well as the calibration beads. Control samples including only primary or secondary antibody were prepared with set up beads. As described in the manufacturer's protocol, a standard curve was performed with different mean fluorescent intensities (MFI) provided with the calibration beads to calculate the specific number of molecules of CD20 and CD22 on the surface of Raju and Daudi cell lines.

Cytotoxicity assay

Target cell lines (Raji or JeKo1 cells) were cultured in a 96-well plate at 10,000 cells per well in complete OpTmizer media without IL2 and CAR T cells or nontransduced control T cells (NTD) were added at different ratios (10,000 to 100,000 CAR-positive cells). Cocultures were cultivated at 37°C, 5% CO_2 overnight. Next day, ONE-Glo reagent was prepared following the manufacturer's instructions (Promega, #E6120). And 50 μL of ONE-Glo reagent was mixed at a 1:1 ratio with target:effector cells in a white, flat-bottom plate. Plate was incubated for 3 minutes at room temperature and luminescence was measured in a FLUOstar Omega microplate reader (BMG Labtech).

The following calculations were used to estimate the percentage of lysis:

%Lysis = (1 − ((luminescence CAR against tumor cells/luminescence NTD against tumor cells)/(luminescence CAR against control cells)/(luminescence NTD cells against control cells)))*100

or % Lysis = (1 − CAR sample luminiscence/NTD luminiscence)* 100 if no double-negative cell line was available.

Flow cytometry

For CAR expression analysis, transduced dual CAR cells were stained using a two-step procedure. Briefly, cells were first incubated with the extracellular domain of the CD22 protein fused to the Fc domain of mouse IgG1 [Lake Pharma (26, 27)] and with a His-tagged CD20 protein (ACRO Biosystems, #CD0-H52H3-20 mg; Supplementary Fig. S2) in FACS buffer (PBS + 3% FBS + 0.1% sodium azide). After washing in FACS buffer, cells were incubated with a Cy™3 AffiniPure Goat Anti-Mouse IgG (Jackson ImmunoResearch, 115-165-205; RRID: AB_2338694) and an anti-His antibody coupled with APC (BioLegend, 362605; RRID:AB_2715818). To costain to assess the efficiency of gene editing, cells were subsequently incubated with anti-CD4 APC-Vio770 (Miltenyi Biotec, 130-113-211; RRID: AB_2726022), anti-CD8 Vioblue (Miltenyi Biotec, 130-110-683; RRID:AB_2659239), anti-TCRαβ PE-Vio770 (Miltenyi Biotec, 130-119-617; RRID:AB_2733284), and anti-CD52 AF488 (BD Bioscience; RRID:AB_2738314). For differentiation and exhaustion analysis, 10^5 to 3×10^5 cells CAR T cells were stained in 96-well plates using the antibodies noted in Supplementary Table S2 diluted in FACS buffer for 30 minutes at 4°C.

For bone marrow (BM) analysis at the end of the disseminated lymphoma study described below, NSG mice were humanely sacrificed and the femur was dissected. BM cells were isolated by centrifugation at 7,000 rpm for 1 minute into an Eppendorf tube. To isolate spleen cells, spleens were dissociated with a syringe pestle in PBS with 3% PBS and passed through a 0.45 μm strainer. After that, spleen cells were collected by centrifuging at $300 \times g$ for 5 minutes. For both organs, red blood cells were lysed with BD Pharm Lyse lysing solution (eBioscience, 555899) following the manufacturer's instructions and removed by centrifugation. A total of 1×10^6 cells were stained in lysis buffer in a 96-well plate using the antibodies noted in Supplementary Table S2 for 30 minutes at 4°C.

For all flow cytometry applications, cells were washed in FACS buffer and fixed in 2% formaldehyde before data collection on BD Canto II cytometer using BD FACS DIVA software v9.0. Data analysis was performed using FlowJo Software v10. For Supplementary Fig. S6, Novocyte Penteon Cytometer and NovoExpress V1.6.1 software from Agilent were used for flow cytometry, analysis, and calculation of absolute counts.

TCR depletion

To isolate TCRαβ-negative cells, CAR T cells were incubated with 1,875 μL of TCRαβ biotin antibody (Miltenyi Biotec, 130-113-537) per 10^7 cells for 30 minutes in PBS with 0.5% FBS and 2 mmol/L ethylenediaminetetraacetic acid (EDTA). After that, cells were washed in PBS with 0.5% FBS and 2 mmol/L EDTA and posteriorly incubated with 3.75 μL of anti-biotin magnetic bead per 10^7 cells for 30 minutes (Miltenyi Biotec, 130-090-485) at room temperature. After washing with PBS with 0.5% FBS and 2 mmol/L EDTA, cells were resuspended in 500 μL PBS with 0.5% FBS and 2 mmol/L EDTA and purified using an LD columm (Miltenyi Biotec, 130-042-901) following manufacturer's protocol.

IFNγ secretion assay

The levels of INFγ were evaluated in supernatants obtained from 1:1 effector:target ratio overnight cocultures of CAR T cells:tumor cells using the Human IFN-Gamma Quantikine Kit (R&D Systems, SIF50) following the manufacturer's instructions. Experimental samples contained 50,000 CAR T cells and 50,000 tumor cells were cultured in a total of 100 μL of OpTmizer media with 5% human serum. As positive control, CAR T cells were activated with 1 μmol/L Ionomycin (Sigma-Aldrich, I0634) and 20 ng/mL phorbol 12-myristate 13-acetate (PMA; Sigma-Aldrich, P8139). As negative control, nonstimulated cells and CD20/CD22-negative Raji cells were used.

Serial killing assay

To assess cytolytic activity of CD20xCD22 CAR T cells over time, a serial killing assay was performed following previous protocols (28).

Briefly, dual CAR T cells were mixed with a suspension of Raji-luc cells at a 1:1 ratio in IL2-free complete OpTmizer media. The mixture was incubated for 72 hours before determining the luminescence of 25 μL of cell suspension using 25 μL of ONE-Glo reagent as described above (see *Cytotoxicity Assay*). The cell mixture was then spun down, and the old media was discarded and substituted with Raji cells in fresh media. The resulting cell mixture was incubated for 72 hours. This protocol was repeated for up to 11 days. At the end of the experiment, cells were incubated with the antibody panels noted on Supplementary Table S2.

In vivo experimentation

All procedures involving animals at Mispro-Biotech and Invivotek were performed in accordance with regulations and established guidelines of the Animal Ethical Committee and were reviewed and approved by the Institutional Animal Care and Use Committee at Mispro-Biotech. The patient-derived xenotransplantation (PDX) study performed at Charles River Laboratories (CRL) was conducted according to all applicable international, national, and local laws and followed the national guidelines for the Care and Use of Laboratory Animals of the Society of Laboratory Animal Science (GV-SOLAS). The protocol was approved by the regional council Committee on the Ethics of Animal Experiments.

Subcutaneous lymphoma model

Immunodeficient NSG mice (NOD.Cg-*Prkdc*^{scid} *Il2rg*^{tm1Wjl}/SzJ, the Jackson Laboratory), were received and acclimatized. NSG mice (6–7 weeks old, female) were then injected with 0.5×10^6 Raji (ATCC #CCL-86; RRID:CVCL_0511) tumor cells in matrigel (Corning, CB-40234C) on each flank subcutaneously. Mice were randomized after day 7 based on average tumor growth, which was measured using bioluminescence imaging (BLI). Next day, mice were adoptively intravenously transferred with the different CAR T-cell groups (8×10^6 and 3×10^6 CAR-positive cells for dual CAR T cells, 8×10^6 CAR-positive cells for single CAR T cells, 8×10^6 NTD). Mice were imaged at the indicated times with 15 mg/mL BD Monolight D-Luciferin (BD Biosciences, 556888) injected intraperitoneally following manufacturer's protocol and monitored for survival. Images were analyzed with IVIS Perkin Elmer software and average radiance was represented to monitor tumor growth.

Disseminated lymphoma models

Immunodeficient NSG mice (6–7 weeks old, female) were intravenously injected with Daudi-Luc-GFP tumor cells (0.5×10^6 cells per animal in 100 μL of PBS). A total of 6 days later, bioluminiscence was measured and mice were randomized. Next day, the indicated CAR-positive T cells were administered for the different groups (10×10^6, 3×10^6, and 1×10^6 for the dual CAR and 10×10^6 for the single CAR and 10×10^6 for the NTD). Daudi-Luc-GFP tumor cell growth was monitored by BLI as described above. Images were analyzed with IVIS Perkin Elmer software and photons/second was represented to monitor tumor growth. Experiments were discontinued at day 60. This experiment was performed at Invivotek.

A second disseminated lymphoma study was performed at Mispro Biotech facility where, 6 to 8 weeks old female NSG mice were injected with Daudi-Luc-GFP tumor cells (0.5×10^6 cells i.v. per animal in 100 μL of PBS). A total of 6 days later, bioluminiscence was measured using an IVIS Spectrum In Vivo Imaging System (Perkin Elmer) and mice were randomized. Next day, 3 million CAR-positive T cells of the single CD22 CAR or either version of the dual CAR were administered. Daudi-Luc-GFP tumor cell growth was monitored by BLI, and surviving animals were sacrificed on day 105 when the BM was analyzed as described in the flow cytometry method section.

Primary B-NHL samples thawing and phenotyping

Primary B-NHL samples from either BM or peripheral ganglia ($n = 21$) were obtained from the biobank at the Hospices Civils de Lyon, France (https://www.chu-lyon.fr/centre-de-ressources-biologiques), where written informed consent from patients was obtained in accordance with the French public health code (Code de la Santé Publique -CSP-). The operations of the biological resource center for the Hospices Civil de Lyon in in compliance with French legislation (Bioethics law of August 2004). They abide by all regulatory and ethical requirements in compliance with internationally recognized standards that rule collection, conservation and use of biological samples for scientific purposes. Samples were cryopreserved and stored and the Center for Biological Resources (Centre des Ressources Biologiques -CRB-) of the Hospices Civils de Lyon prior to transferring to Cellectis facilities, where they were stored at −150°C. *In vitro* studies performed at Cellectis were reviewed and approved by the High Council of Biotechnology (Haut Conseil des Biotechnolgies -HCB-), from the Ministry of Education, Research & Innovation in France. Cells were thawed in 20 mL of OpTmizer media supplemented with 10% FBS in the presence of 0.4 μL of Benzonase (E1014-5KU- Sigma-Aldrich). Cells were washed and resuspended in 10 mL of media. Cells were stained with eFluor 780 fixable viability dye (eBioscience, 650865) for 20 minutes at 4°C in a 96-well plate and washed with 100 μL PBS/2% FBS per well. Then samples were incubated with Fc Block reagent (Miltenyi Biotec, 130-059-901) for 10 minutes at 4°C and then incubated with the mixture of antibodies noted in Supplementary Table S2 in BD Horizon brilliant stain buffer (BD Biosciences, 563794) for 20 minutes at 4°C. Data collection on BD Canto II cytometer using BD FACS DIVA software v9.0. Data analysis was performed using FlowJo Software v10.

Primary B-NHL cytotoxic activity

A total of 50,000 total cells from the primary B-NHL samples were incubated with dual CAR T cells at different effector:target ratios (1:1, 5:1, 10:1) in RPMI1640 GlutaMAX (Thermo Fisher Scientific, 61870-044) supplemented with FBS and Penicillin/Streptomycin for 17 hours at 37°C. As negative control, MOLM-13 cells were used. After incubation, cells were washed with PBS and stained with e780 fixable viability dye (eBioscience, 65-0865) at 1:1,000 concentration for 20 minutes at 4°C, after washing Fc block was added and incubated for 10 minutes at 4°C, cells were centrifuged and incubated with the antibodies indicated in Supplementary Table S2 in PBS with 2% FBS. Cells were finally resuspended in 100 μL of 2% formaldehyde with 20 μL of countbright absolute cell counting beads (Invitrogen, C36950). Viability was evaluated by flow cytometry on a CANTO II instrument (Becton Dickinson) and using a Flojo V10 software for analysis and the % of specific lysis (cytotoxic activity) was calculated as:

Specific lysis = 1 − [(% viable B-NHL cells with CAR)/(% viable B-NHL cells without CAR)]/[(%viable MOLM-13 with CAR)/(% MOLM-13 viable cells without CAR)].

PDX assays

The PDX study was performed at CRL, Discovery Research Services Germany GmbH. Mantle cell lymphoma (MCL) PDX had been generated at CRL (LYPDX2894) from primary lymph node. Patient informed consent in accordance with the current German legislation and in compliance with internationally recognized

standards was obtained by CRL, Discovery Research Services Germany GmbH, Freiburg.

For tumor generation, lymphoma cells were obtained from the spleens of donor mice. The spleen was excised after euthanasia and placed in a falcon tube filled with 15 mL medium. It was strained through a 100 μm cell strainer to obtain single cells, a red blood cell lysis was performed with ammonium-chloride-potassium (ACK) buffer (150 mmol/L ammonium chloride, 10 mmol/L potassium bicarbonate, 0.1 mmol/L EDTA, pH 7.2–7.4) and incubating for 1 to 3 minutes at room temperature. Cells were pelleted by centrifugation at 300 × *g* for 5 minutes at room temperature. Mouse cells were removed by using a mouse cell depletion kit (Miltenyi Biotec #130-104-694) according to the manufacturer's instructions and the remaining cells were counted and resuspended in PBS. Collected lymphoma cells were orthotopically implanted (intrasplenic) in female NSG mice ages 5 to 9 weeks. Recipient animals were given an analgesic drug [2 mg/kg butorphanol (Morphasol) at 10 mL/kg s.c.] 30 minutes prior to implantation. The animals were anesthetized by inhalation of isoflurane and 3×10^6 lymphoma cells in 30 μL PBS were injected into the spleen. After the procedure, animals received the analgesic drug carprofen at 5 mg/kg s.c. every 12 to 24 hours until no symptoms of pain were observed, for a maximum of 3 days. Mice were examined daily and scored for their level of activity and their behavior. Termination of animals was performed on the basis of CRL animal welfare policies/ethical endpoints. A total of 21 days after tumor implantation, 30 mice were randomized into five groups of 6 animals based on bodyweight and treated with either vehicle, 10×10^6 TCRαβ knockout cells, 1×10^6, 3×10^6 or 10×10^6 UCART20x22 cells. Peripheral blood (PB) samples were taken at D3, D20, and at the end of the experiment (D70). Spleen and BM samples were also harvested upon sacrifice. Animals were sacrificed when signs of distress were observed, according to the activity and behavior scores defined by CRL. Samples were stained with anti-mouse CD45 (clone 30-F11 BioLegend, catalog no. 103127; RRID:AB_493714), anti-human CD45 (clone HI30 BioLegend, 304029, RRID:AB_2174123), and anti-human CD19 (clone HIB19 BioLegend, 302218; RRID:AB_314248) to identify human cells and discriminate tumor cells from CAR T cells.

Cytokine secretion assay

The levels of released cytokines *in vivo* were evaluated in mouse plasma samples collected at D3 and D20 using the LEGENDplex Human Th Cytokine Panel (BioLegend, 741027) according to the manufacturer's instructions.

Statistical analysis

For statistical analysis, Graph Pad Prism 9 was used. Thresholds for *P* value were: *, <0.05; **, <0.01; ***, <0.001; ****, <0.0001. For multiple comparisons, Tukey correction was used when indicated.

Data availability

The data generated in this study are available in the article and its Supplementary Data or upon request from the corresponding authors.

Results

Dual CAR T cells efficiently eradicate CD20$^+$ and CD22$^+$ tumors

Different methodologies have been explored for the generation of dual CAR T cells. Some mix two individual CAR constructs to either cotransduce or generate a mixed CAR T-cell product, and others use a single construct to deliver both CARs simultaneously as a tandem or a bicistronic construct (29). Here, we engineered two versions of allogeneic dual CAR T cells simultaneously targeting CD20 and CD22 using bicistronic cassettes, CD20xCD22 CAR (refers to both versions of the dual CAR tested in this study; refs. **Fig. 1A** and **B**). Each of the CARs carried a CD8α hinge and transmembrane domain as well as a 4-1BB costimulatory domain and the CD3ζ activation domain. 4-1BB signaling has been previously shown to increase CAR T-cell persistent activity in autologous settings (30). The coding sequences of the CD20 and CD22 targeting CARs were separated by a P2A ribosomal skip peptide to enable simultaneous expression of both CARs in the same cell. The CD22.CD20CAR version harbors the CD22 CAR coding sequence in the first position, while the CD20.CD22CAR version contained the CD20 CAR coding sequence in the first position. As positive controls, we used a single CD22 CAR (CD22CAR) and a single CD20 CAR (CD20CAR). CAR expression was driven by the EF-1alpha promoter, currently being used in the clinic and shown to display high efficiency for surface CAR expression (31, 32). Dual allogeneic CAR T cells also contained two TALEN-mediated gene knockouts (**Fig. 1A**): *TRAC*, to prevent GVHD, and *CD52*, to render the CAR T cells resistant to anti-CD52 lymphodepleting agents such as alemtuzumab and, thus, allow a deeper and longer lymphodepletion to facilitate allogeneic CAR T-cell engraftment and persistence. We have previously shown that *TRAC*/*CD52* double knockout can efficiently and reproducibly allow manufacturing of "off-the-shelf" CAR T cells (33). Of note, ongoing clinical studies are demonstrating safety and efficacy of allogeneic CAR T cells directed against other targets manufactured using the same platform (13, 17, 34, 35).

In this study, CAR T cells were generated using PBMCs from healthy donors. T cells were activated using CD3/CD28 beads, transduced with the relevant recombinant lentiviral vector, and subsequently transfected with mRNA encoding TALEN targeting *CD52* and *TRAC* genes. After expansion of the engineered cells at small scale, we analyzed CAR expression by flow cytometry and demonstrated that both allogeneic dual CAR T-cell versions allowed concurrent CD22 CAR and CD20 CAR expression at the cell surface (**Fig. 1C**). Transduction efficiencies ranged from around 10% to 60% at the end of the process in the samples evaluated (Supplementary Fig. S3A). The bicistronic construct showed a slightly lower MFI for the CD22 CAR, while we did not observe differences on CD20 CAR expression between the bicistronic and the single construct at day 8 after transduction (Supplementary Fig. S3B). Similarly, we showed that TALEN treatment efficiently knocked-out *TRAC* and *CD52* genes (Supplementary Fig. S3C and S3D). To ensure safety in the clinic, remaining TCRαβ-positive cells can be efficiently depleted using a clinical-grade available magnetic depletion system (Supplementary Fig. S3E and S3F), as it has been previously shown (36).

Simultaneous delivery of both CARs in one construct has been proposed to facilitate manufacturing (37), and we evaluated if this was the case for the CD20 and CD22 CARs used in this preclinical study. For that, we compared the transduction of the bicistronic constructs versus cotransduction of the two single constructs at different MOIs. These experiments showed that regardless of the MOI used, the percentage of cells expressing the dual CAR was higher with a bicistronic construct than with two individual constructs (Supplementary Fig. S4A and S4B).

On the basis of these results, we focused on comparing both bicistronic constructs and benchmarking them against the single CAR constructs. For this purpose, we mostly used single CD22 CAR because transduction efficiencies were higher. We first evaluated key T-cell features via flow cytometry and demonstrated that transduction with the dual CAR construct did not alter the CD4/CD8 ratios

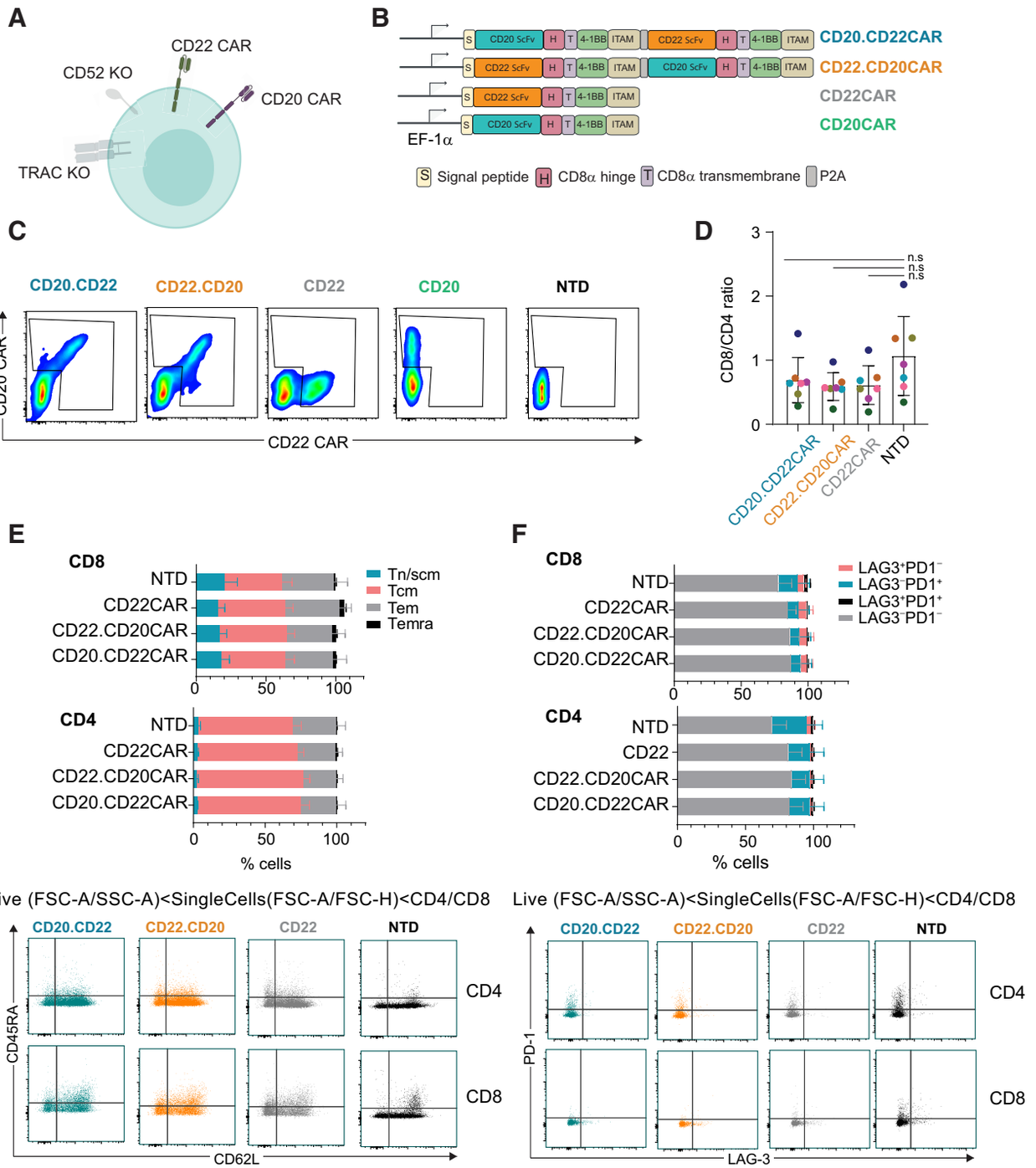

Figure 1.

CD20xCD22 CAR T cells can be efficiently generated. **A,** Diagram showing CD20xCD22 CAR T cells including all attributes. **B,** Dual and single CAR T-cell constructs used in this study. **C,** Flow cytometry data showing CAR expression for dual and single CAR T cells (representative diagram of $n = 6$–15 from four independent experiments). **D,** Ratio of CD8/CD4 cells in the productions indicated. Mean ± SD is shown. **E,** Flow cytometry data showing differentiation status of CAR T cells expressing the indicated CAR constructs. Tn/scm: naïve T cells ($CD45RA^+CD62L^+$); Tcm: central memory T cells ($CD45RA^-CD62L^+$); Tem: effector memory T cells ($CD45RA^-CD62L^-$); Temra: effector memory T cells RA ($CD45RA^+CD62L^-$). Representative dot plots are shown below. **F,** Expression of exhaustion markers PD-1 and LAG-3 in $CD8^+$ and $CD4^+$ cells from CD20xCD22 CAR at the end of production. Representative dot plots are shown below. $N = 7$ from three independent experiments for both **E** and **F**. Mean ± SEM is represented. One-way ANOVA was performed with Tukey correction for multiple comparisons was perfomed and no significant differences were identified.

compared with nontransduced cells (**Fig. 1D**; Supplementary Fig. S3G). Similarly, phenotypic analysis of differentiation and exhaustion markers revealed low levels of differentiation and exhaustion, which were comparable with the values obtained in the nontransduced controls (**Fig. 1E** and **F**). Altogether, these data show that dual CAR T cells can be efficiently generated from healthy donor PBMCs using a CD20xCD22 bicistronic construct while preserving T-cell characteristics.

CD20xCD22 CAR T cells exhibit potent *in vitro* cytolytic activity

To assess the activity of dual CAR T cells, we performed luciferase-based *in vitro* cytotoxicity assays by incubating CD20xCD22 CAR cells with Raji cells (a Burkitt lymphoma tumor cell line expressing both CD20 and CD22 antigens) at different effector:target ratios. These experiments demonstrated that T cells expressing either of the versions of the CD20xCD22 CAR efficiently killed tumor B cells in a dose-dependent manner (**Fig. 2A**; Supplementary Fig. S5A). These results were confirmed with other cell lines, such as Jeko-1, a MCL line expressing CD20 and CD22 (Supplementary Fig. S5B and S5C). We then evaluated the response of dual CAR T cells to the emergence of antigen escape, and for that, we engineered Raji cells to express a single antigen using specific TALEN against either *CD20* or *CD22* (Supplementary Fig. S5D and S5E). As shown in **Fig. 2B** and **C** and Supplementary Fig. S5F, dual CD20xCD22 CAR T cells potently lysed tumor cells expressing a single target, while each of the single CARs did not show cytotoxic activity against Raji cells that did not express their specific target antigens. This highlights the ability of dual CAR T cells to target a broader spectrum of tumor cells expressing different antigen combinations.

To evaluate cytokine release upon antigen recognition, we measured IFNγ production after incubating CD20xCD22 CAR cells overnight with tumor cells expressing different antigen combinations. As **Fig. 2D** shows, exposure of the dual CAR T cells to antigen triggered a specific cytokine response that was comparable for both versions of the CD20xCD22 CAR tested (**Fig. 2D**; Supplementary Fig. S5G). Response to the CD20 antigen elicited secretion of higher amounts of IFNγ cytokine, which could be attributed to a higher amount of CD20 molecules expressed in Raji cells compared with CD22 (Supplementary Fig. S4D and S4E). All cells, including nontransduced control, released IFNγ upon PMA and Ionomycin activation (Supplementary Fig. S5H). In contrast, no IFNγ was observed upon incubation with $CD20^{-}CD22^{-}$ cells, demonstrating the absence of target-independent activation. Altogether, these results show that dual CAR T cells exert specific cytolytic activity against double-positive or single antigen–positive tumor cells.

Tumor-associated CD20 and CD22 persistently drive CD20xCD22 CAR T-cell cytolytic activity and proliferation

Having confirmed antigen-dependent cytotoxic activity for the dual CAR T cells *in vitro*, we evaluated whether CD20xCD22 CAR T cells displayed sustained CAR activity and proliferation after repeated exposure to tumor over time. We used serial killing experiments, in which we exposed CD20xCD22 CAR T cells to fresh Raji cells every 3 days (**Fig. 2E**). In addition, to evaluate the activity of the dual CAR T cells in the presence of a single antigen, we performed the same experiments with Raji cells engineered to express a single antigen ($CD20^{+}CD22^{-}$ or $CD20^{-}CD22^{+}$). As shown in **Fig. 2F**, CAR T cells efficiently and persistently eradicated double-positive tumor cells over time. Moreover, compared with the single CAR T cells, the dual CAR T cells displayed similar robust cytolytic activity over time against tumor cells expressing a single antigen, validating the benefit of using a dual CAR approach (**Fig. 2G** and **H**). Flow cytometry analysis at the end of the 2 weeks of repeated exposure of CAR T cells to the tumor, showed enrichment of CAR^{+} cells (Supplementary Fig. S6A) and complete eradication of tumor cells with both versions of the CD20xCD22 CAR (Supplementary Fig. S6B and S6C). In addition, we evaluated the T-cell characteristics at the end of the serial killing assay and did not identify any differences between T cells engineered to express either of the biscistronic constructs when exposed to Raji cells expressing a variety of antigen as indicated (**Fig. 2I**–**K**; Supplementary Fig. S6D). As expected, the lack of CD22 antigen failed to activate single CD22 CAR T cells and trigger continuous tumor cell lysis (**Fig. 2H** and **K**).

We also evaluated the proliferation of the CAR T cells and observed that after 14 days of repeated exposure to antigen (Supplementary Fig. S7A), T cells engineered to express either of the dual CARs continued to proliferate when exposed to Raji cells expressing two or one antigens (Supplementary Fig. S7B–S7D). At day 14, T cells expressing either of the single CARs showed less tumor control activity when cultured with single antigen–expressing Raji cells. We also observed a higher level of activation for the dual CAR T cells when tumor cells presented both antigens, as indicated by expression of the IL2 receptor alpha, CD25 (Supplementary Fig. S7E and S7F). Analysis of exhaustion markers PD1, TIM3, and LAG3 showed no striking differences between the samples evaluated, suggesting that none of the conditions tested in this study lead to dysfunctional T cells (Supplementary Fig. S7G and S7H). Altogether, these experiments demonstrate that dual CAR T cells have a higher potential for persistent response to antigen-specific stimulation and robust tumor-cell killing activity against different combinations of antigen-expressing tumor cells.

CD20xCD22 CAR T cells efficiently eradicate tumor burden *in vivo* in a dose-dependent manner

Next, we evaluated the antitumor activity of dual CAR T cells and compared both bicistronic constructs *in vivo* using a disseminated Burkitt lymphoma model (Daudi cells) in which the cells were engineered to express luciferase. *NOD.Cg-Prkdcscid Il2rgtm1Wjl/SzJ* (NSG) mice received intravenous administration of tumor cells and were treated 7 days later with different doses of T cells engineered to express either of the versions of the CD20xCD22 CAR or nontransduced T cells as control (NTD; **Fig. 3A**). Tumor burden was monitored overtime by BLI (**Fig. 3B** and **C**). While animals treated with PBS or NTD cells succumbed to disease within 3 weeks, cohorts treated with T cells engineered to express either of the dual CARs survived until the end of the study (**Fig. 3D**). Moreover, we demonstrated that T cells engineered to express either of the CD20xCD22 CAR versions potently targeted tumor cells *in vivo* in a dose-dependent manner (**Fig. 3B**), with doses of 3 and 10 million CAR T cells achieving complete tumor clearance. Early responses at a dose of 10 million CAR T cells resulted in stronger tumor clearance with the dual CAR than the single CAR. Treatment with a low dose of 1 million CAR T cells was sufficient for tumor clearance and it was stronger with the CD20.CD22CAR version. In addition, we performed a parallel *in vivo* study where the animals were treated with 3 million single and dual CAR T cells. We observed a significant advantage in tumor clearance and animal survival for both dual CAR versions (Supplementary Fig. S8A and S8B). We also analyzed the BM and spleen of the surviving animals

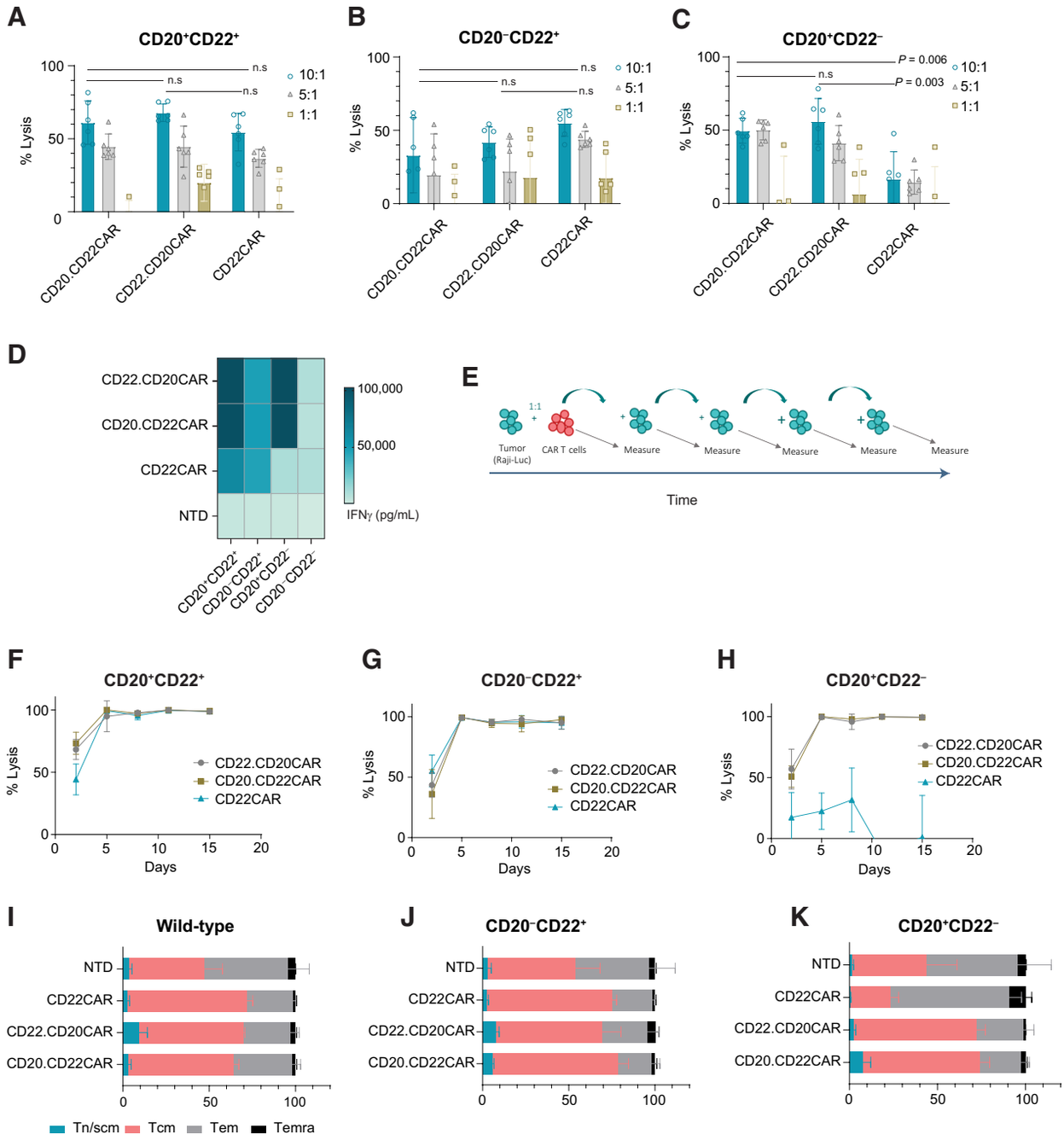

Figure 2.

CD20xCD22 CAR T cells display robust activity against tumor cells with different antigen expression. **A,** Representative cytotoxic activity against Raji (Burkitt lymphoma) cells expressing $CD20^+CD22^+$. **B** and **C,** Cytotoxic activity against Raji cells expressing $CD22^+$ or $CD20^+$. $n = 6$. Mean ± SD shown. Unpaired t test was performed. The experiment was repeated three times each with 2 or 3 different donors. **D,** Heat map showing IFNγ release after overnight incubation at an effector: target ratio of 1:1. The experiment was repeated three times each with 2 or 3 different donors. **E,** Serial killing assay schematics. **F–H,** Serial killing assay against $CD20^+CD22^+$, $CD22^+$, or $CD20^+$ Raji cells at an effector:target ratio of 5:1. Mean ± SD shown. **I–K,** Flow cytometry data showing differentiation status of CAR T cells at the end of the serial killing assay. Tn/scm: naïve T cells ($CD45RA^+CD62L^+$); Tcm: central memory T cells ($CD45RA^-CD62L^+$); Tem: effector memory T cells ($CD45RA^-CD62L^-$); Temra: effector memory T cells RA ($CD45RA^+CD62L^-$). Mean ± SD shown. $n = 3$.

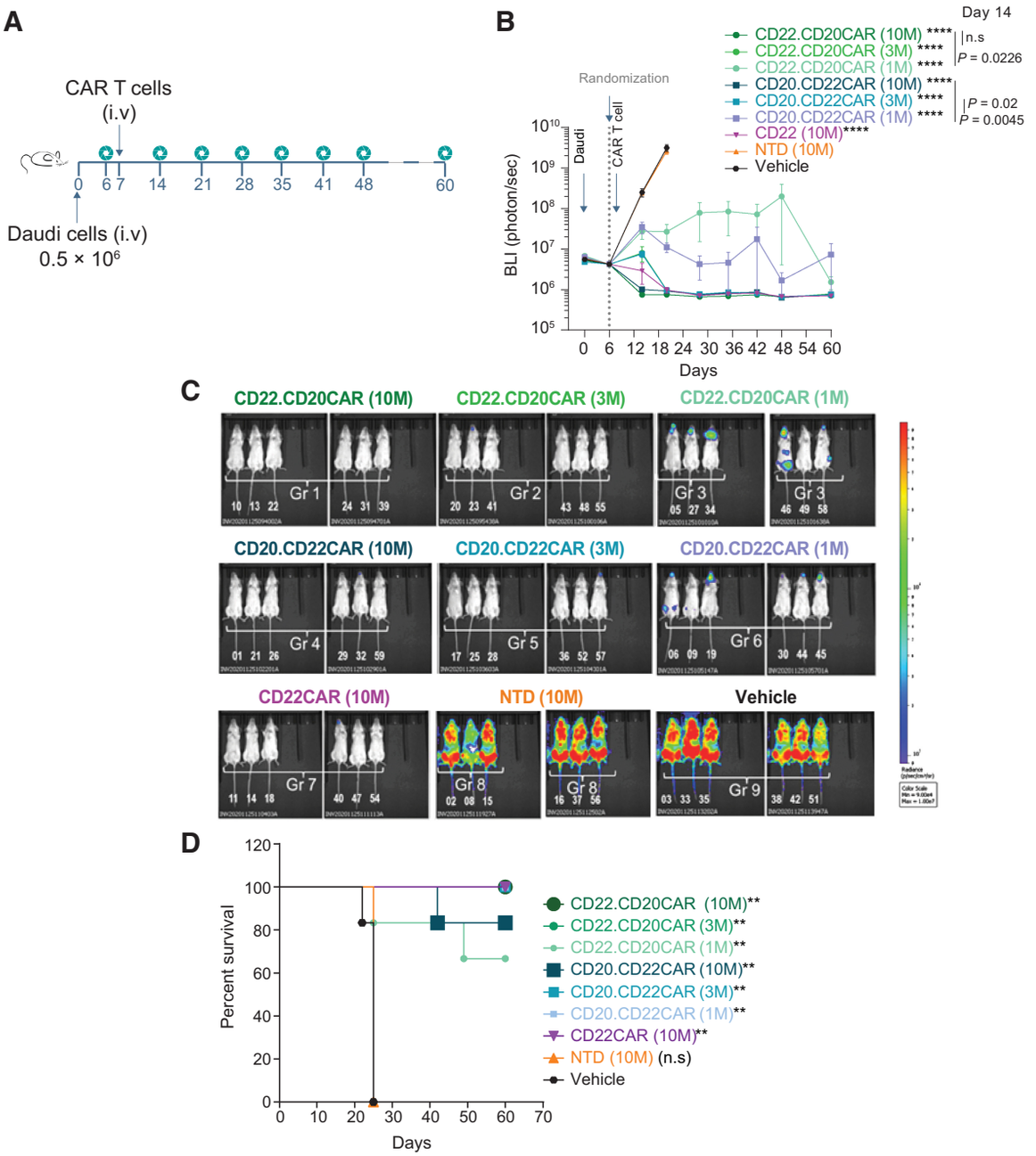

Figure 3.

CD20xCD22 CAR T cells display robust tumor control activity in a dose-dependent manner *in vivo*. **A,** Schematics showing the design of the disseminated lymphoma model study with Daudi cells. **B,** Tumor growth control overtime after tumor implantation and CAR T-cell treatment with the indicated constructs using intravenously administered Daudi cells, $n = 6$ per condition. One-way ANOVA was performed with Tukey correction. Mean ± SEM is shown. **C,** Representative bioluminescence ventral at day 20 of the study. **D,** Kaplan–Meier curves showing survival of NSG animals treated with different versions of CD20xCD22 CAR and CD22 CAR T cells. Log-rank Mantel–Cox test was calculated for survival curves. Significant values are indicated. *P* value definition: *<0.05, **<0.01, ***<0.001, ****<0.0001.

treated with the dual CAR T cells at the end of the study. This analysis revealed that dual CAR T cells efficiently eradicated the tumor and also persisted in the BM for longer than 100 days (Supplementary Fig. S8C and S8D). Moreover, no tumor could be detected at this point, underscoring the robustness of the dual CAR T cells.

CD20xCD22 CAR is a suitable approach to address antigen escape

Upon confirming the potent activity of the dual CAR T cells *in vivo*, we mimicked tumor antigen escape *in vivo* using a subcutaneous model of Burkitt lymphoma with Raji cells. In this model, three different tumors (double-positive $CD22^{+}CD20^{+}$, single-positive

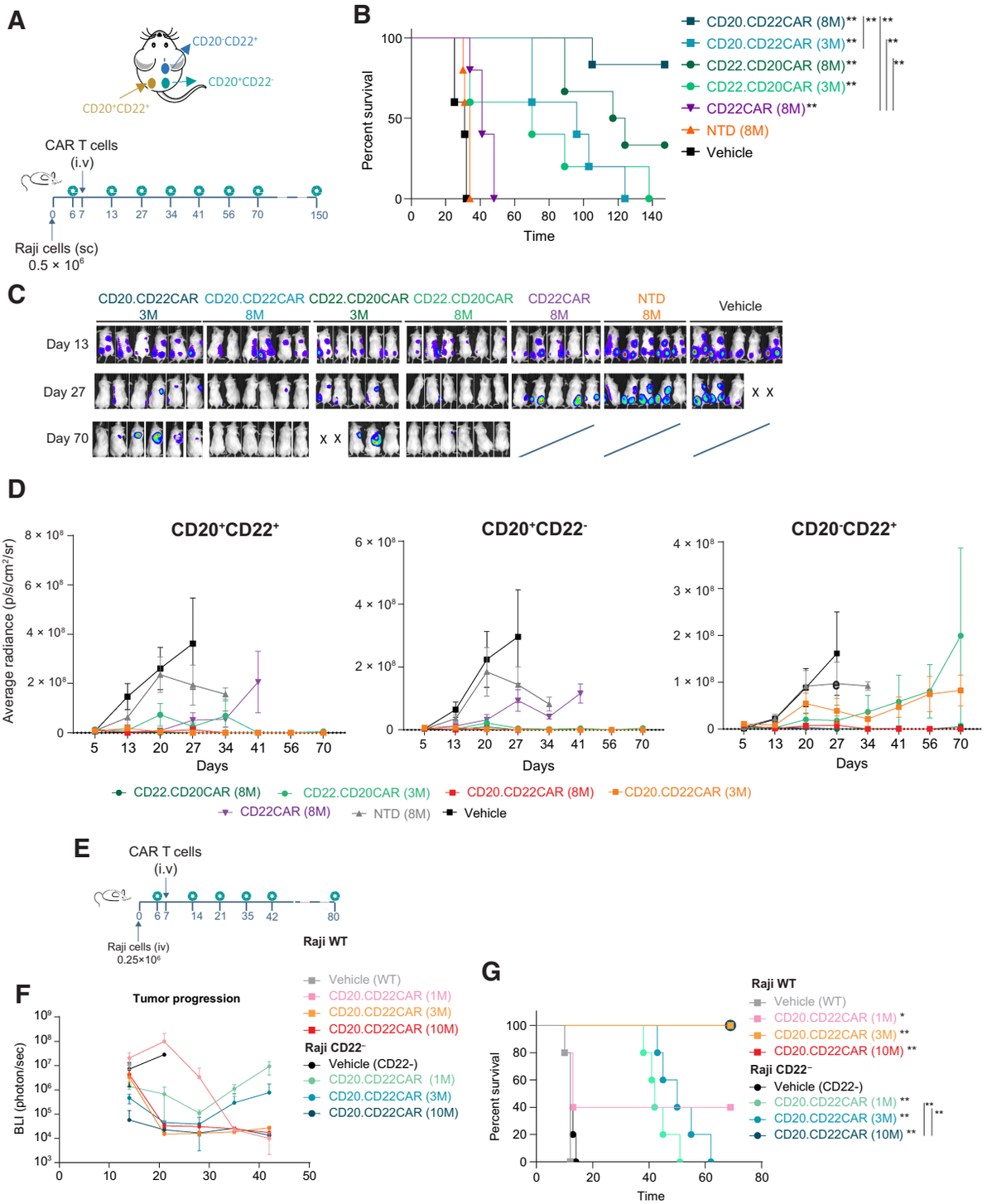

Figure 4.

Efficient *in vivo* activity exerted by CD20xCD22 CAR T cells against different combinations of antigen-expressing cells in an aggressive lymphoma model. **A,** Schematic showing tumor model experimental design with NSG mice injected subcutaneously with Raji cells (Burkitt lymphoma). **B,** Kaplan–Meier curves showing survival of NSG animals with subcutaneous Raji tumors treated with different versions of CD20xCD22 CAR and CD22 CAR T cells ($n = 3$–6). **C,** BLI of tumors of NSG mice treated with indicated CAR T cells and measured at different timepoints. **D,** Graphs measuring of growth of $CD20^+CD22^+$, $CD20^+CD22^-$, and $CD20^-CD22^+$ tumors, respectively, after treated with the indicated does of CD22.CD20CAR, CD20.CD22CAR, and CD22CAR as indicated. Average radiance (photons/second/cm^2/sr) is shown. **E,** Schematics showing the design of the disseminated lymphoma model study with different Raji cells to model antigen escape. **F** and **G,** Tumor growth control overtime and Kaplan–Meier curves after intravenous administration of Raji tumor cells and CAR T-cell treatment with the indicated constructs ($n = 5$). Statistical value was calculated against vehicle. Log-rank Mantel–Cox test was calculated for survival curves. Significant values are indicated. *P*-value definition: *<0.05, **<0.01, ***<0.001, ****<0.0001. WT, wild-type.

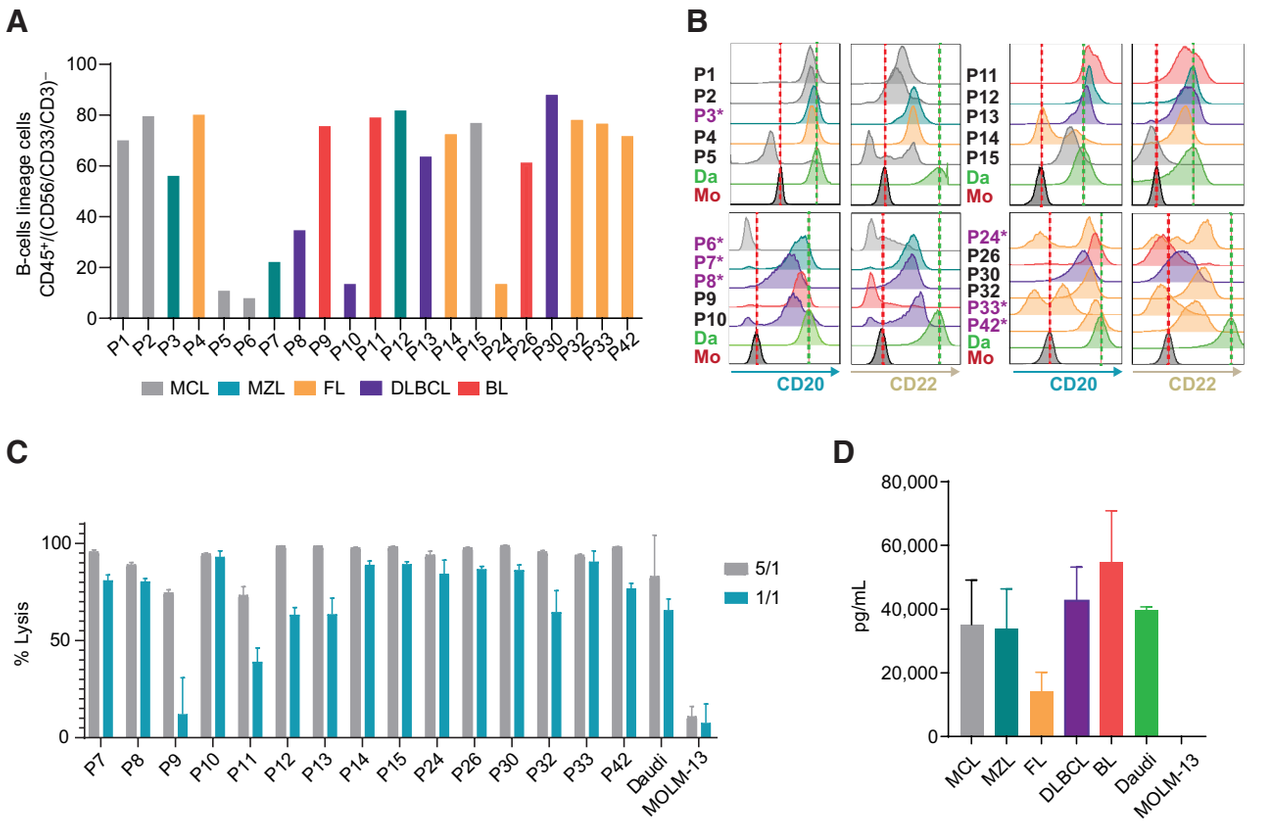

Figure 5.

CD20xCD22 CAR T cells efficiently target primary B-NHL cells. **A,** Graph showing percentage of cells from the B-lineage identified in B-NHL primary samples, defined by %CD45$^+$ cells within CD56$^-$/CD33$^-$/CD3 ($N = 21$). **B,** Flow cytometry data representing the level of CD20 and CD22 expression in samples from **A**. Patients previously treated with rituximab are indicated with an asterisk ($N = 21$). **C,** CD20xCD22 CAR T-cell cytotoxic activity against B-NHL samples. **D,** IFNγ release upon exposure to primary B-NHL cells to CD20xCD22 CAR T cells.

CD22$^+$, and single-positive CD20$^+$) were simultaneously injected in three different flank sites (**Fig. 4A**). Controls treated with NTD cells or PBS succumbed to disease in less than 40 days. CD20xCD22 CAR T-cell treatment efficacy was dose dependent, with animals treated with 8 million CAR T cells showing the longest survival and tumor control (**Fig. 4B**). Animals treated with the single CD22 CAR T cells succumbed to the disease shortly after control animals due to the progression of CD20$^+$CD22$^-$ tumors. We monitored tumor burden individually via BLI over time (**Fig. 4C** and **D**) and showed that both CD20xCD22 CAR T cells efficiently controlled tumor burden regardless of the antigen combination (**Fig. 4D**). These results underscore the benefit of using a dual CAR T cell as it can control a larger diversity of tumors expressing different antigens. In addition, we observed that CAR T cells targeting CD22 exerted low activity against single-antigen CD20$^+$ cells. The low activity observed could be due to the presence of a truncated CD22 protein on the membrane that can still be detected by the CD22 scFV (Supplementary Fig. S8E) and suggest that both the single and the dual CAR could target CD22-low tumor cells.

Furthermore, we studied a disseminated lymphoma model using wild-type Raji cells and single CD20$^+$ expressing cells to recapitulate antigen escape and evaluate dual CAR T-cell cytolytic activity. In this model, tumors were generated via intravenous administration of tumor cells in NSG mice (**Fig. 4E**). We then focused on the CD20. CD22CAR orientation, because it seemed to have a better activity. This study demonstrated that CD20xCD22 CAR T cells efficiently controlled double-positive CD20$^+$CD22$^+$ tumors as well as tumors that had lost CD22 expression (**Fig. 4F**), improving survival in both cases (**Fig. 4G**). Of note, through the different experiments, efficient tumor control was observed with two distinct cell lines, Raji and Daudi, which express different levels of CD20 and CD22, specially CD22 (Supplementary Fig. S5C and S8F). Together, these preclinical data demonstrate that CD20xCD22 CAR T cells efficiently target different combinations and levels of commonly expressed targets in B-NHL.

CD20xCD22 CAR T cells effectively kill primary B-NHL cells with diverse CD20 and CD22 expression levels

The expression levels of CD20 and CD22 were measured in a series of primary samples from patients with B-NHL (Supplementary Table S3; gating strategy is shown in Supplementary Fig S9A) that were used in parallel as targets to evaluate CD20xCD22 CAR T-cell activity. Flow cytometry analysis showed that most samples (16 of 21) expressed both antigens, albeit at variable levels (**Fig. 5A** and **B**). Four of the samples (P9, P15 P26, and P33) showed expression of only one of the targets, while P6 lacked expression of both target antigens. As highlighted with an asterisk in **Fig. 5B**, some of the samples used in this preclinical study came from patients that had previously been treated with rituximab and all but one showed CD20

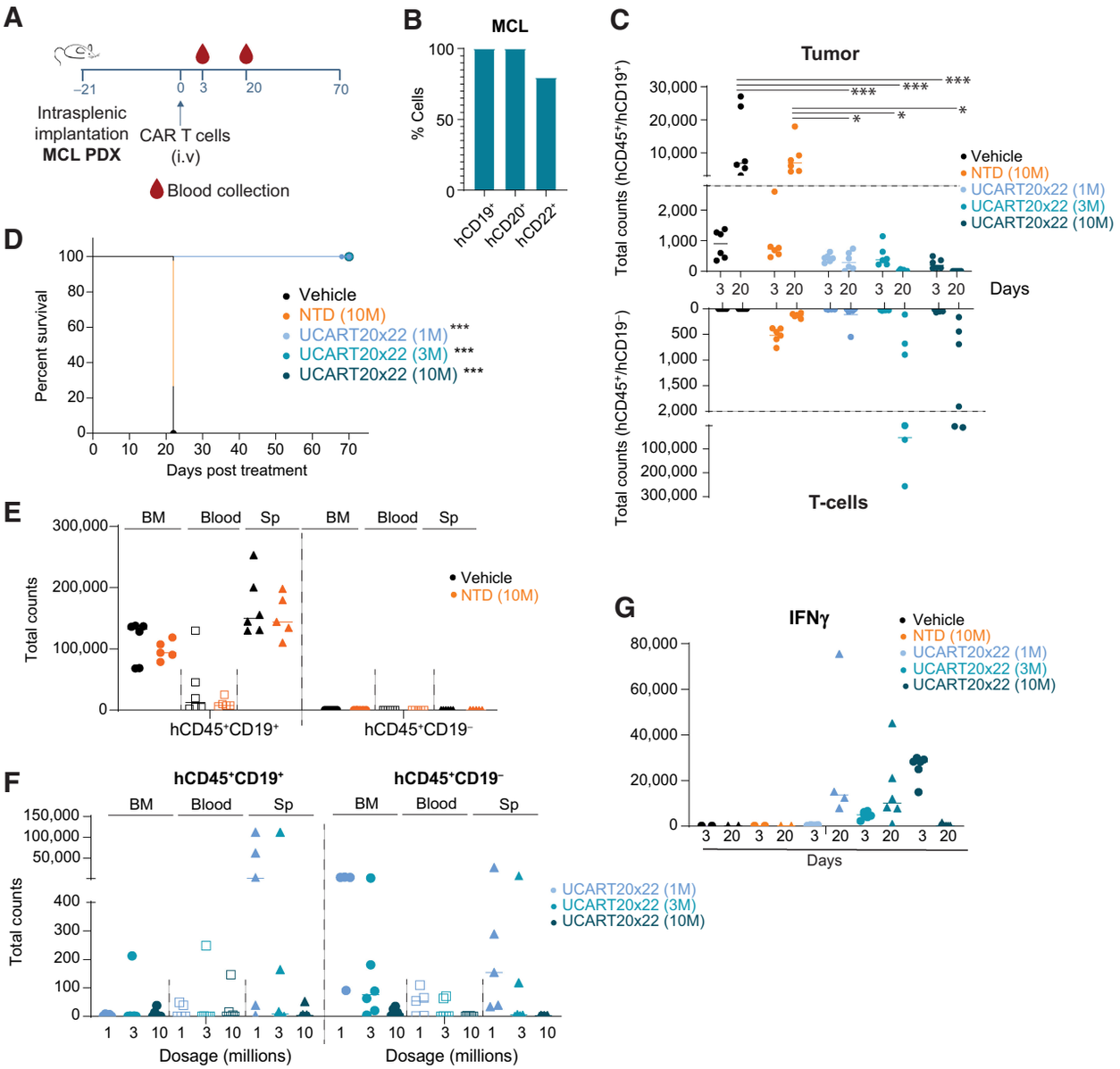

Figure 6.

Patient-derived lymphoma models show improved overall survival upon CD20xCD22 CAR T-cell treatment. **A,** Schematic showing tumor model experimental design with NSG mice injected intrasplenically with primary MCL samples. $n = 6$ per condition. **B,** Levels of CD19, CD20, and CD22 in primary MCL sample. **C,** Graph showing tumor cells and T cells in peripheral blood collected at different timepoints. One-way ANOVA was calculated and significant events are indicated. **D,** Kaplan–Meier curves after intravenous administration of different amounts of CAR T cells in the PDX model. **E** and **F,** Evaluation of tumor cells ($CD45^+CD19^+$ cells) and CAR T cells in the BM, spleen (Sp), and peripheral blood of treated animals at day 22 for vehicle and NTD and day 70 for experimental CAR T-cell treatments. Each dot represents a mouse. **G,** Graph showing IFNγ levels in the plasma of the indicated mice at different days. One-way ANOVA was calculated for experimental samples and no significant events were identified. Log-rank Mantel–Cox test was calculated for survival curves. Significant values are indicated. *P*-value definition: *<0.05, **<0.01, ***<0.001, ****<0.0001.

expression at the time when the samples were retrieved. CD19 levels were also evaluated in a subset of patients and most of the patients showed high numbers of CD19-expressing cells (Supplementary Fig. S9B).

Cytotoxic activity of CD20xCD22 CAR T cells was evaluated with the CD20.CD22CAR orientation against 16 of the 21 B-NHL primary samples available. Potent cytolytic activity was observed in a dose-dependent manner against tumor cells in all samples, indicating that CD20xCD22 CAR can target a broad range of CD20 and CD22 antigen levels, regardless of CD19 expression (**Fig. 5C**). Cytotoxic activity against samples from patients previously treated or not with rituximab was comparable. We did not observe striking differences in the activity

when we compared the cytotoxic activity of the CD20xCD22 CAR T cells among the different subtypes of B-NHL or origins of the sample (Supplementary Fig. S9C and S9D). Furthermore, we evaluated the ability of CD20xCD22 CAR T cells to release the effector cytokine IFNγ in response to antigenic stimulation and compared these responses among the different B-NHL subtypes. For that, the overnight supernatants from 1:1 cocultures of CD20xCD22 CAR T cells with the primary B-NHL samples were harvested and analyzed by ELISA to quantify IFNγ release (**Fig. 5D**). These results showed that CD20xCD22 CAR T cell specifically produced IFNγ upon recognition of the targeted antigens in B-NHL primary samples in all the subtypes of B-NHL tested, but not after exposure to control cell line MOLM-13 ($CD20^-CD22^-$). This dataset indicates that CD20xCD22 CAR T cells can be activated and elicit efficient antitumor activity against a broad spectrum of heterogeneous primary B-NHL samples with various levels of the target antigens.

CD20xCD22 CAR T cells target patient-derived B-NHL *in vivo* leading to improved overall survival

To assess the *in vivo* properties of CD20xCD22CAR T cells in a more physiologically relevant manner, we established a patient-derived xenograft model via intrasplenic implantation using a primary MCL sample expressing CD19, CD20, and CD22 (**Fig. 6A** and **B**). We used different doses of CD20xCD22CAR T cells and as a control *TRAC* and *CD52* gene-edited cells were used. We observed that at day 20 all doses tested exerted strong tumor control, with 3 and 10 million groups leading to complete tumor eradication (**Fig. 6C**; Supplementary Fig. S10). At day 20, a higher number of CAR T cells were detected in animals treated with 3 and 10 million cells. We monitored animal survival until day seventy when the study was terminated and confirmed that all doses evaluated significantly improved overall animal survival (**Fig. 6D**).

Analysis of the animals at the time of sacrifice (22 days for controls and 70 for treated animals) revealed that uncleared tumor cells in the CAR T-cell treated mice mainly resided in the spleen and also in the BM for untreated controls (**Fig. 6E** and **F**). CAR T cells could be found in the spleen, BM and, to a lesser extent, in the peripheral blood for animals treated with 1 and 3 million CAR T cells. These could be due to the presence of remaining tumor cells in these groups. We also evaluated the levels of secreted cytokines *in vivo* upon CAR T-cell administration at day 3 and 20. The main cytokine detected was IFNγ in all CAR T-cell groups in a CAR^+ dose-dependent manner (**Fig. 6G**). All these data together indicate that CD20xCD22CAR T cells clear patient-derived MCL tumors in a dose-dependent manner improving overall survival after lymphoma onset.

Discussion

Despite the formidable success of CAR T-cell therapies in the treatment of B-cell malignancies, long-term studies are uncovering some mechanisms underlying relapse, which can be due to poor T-cell quality or immune escape driven by antigen loss or low expression (38, 39). In these cases, prognosis for patients after relapse is dismal and the availability of effective therapies is limited.

Dual CAR T cells are being investigated in the autologous settings as a solution to address relapses due to antigen escape (40). While initial results are promising (4), more research to identify optimal dual CAR constructs is underway (21). A recent study on a tandem-loop autologous CAR T cell against CD19 and CD22 identified potential limitations due to the configuration of the CAR (41). In preclinical studies, this group explored bicistronic conformations of the CD19/CD22 CAR with promising results. In the context of multiple myeloma, similar studies comparing bicistronic, single, and tandem approaches to prevent BCMA-driven tumor escape demonstrated an advantage for the bicistronic approach versus tandem, when the tumor cells expressed both targeted antigens (42). Another important aspect to consider in the search for dual constructs is that the focus of attention remains on CD19, limiting the choices to treat CD19-low/negative tumors or relapses (6) and indicating the urgent need to develop alternative or complementary CAR T-cell therapies against other targets whose performance can be comparable with CD19 targeting (21). Here, we provide a robust preclinical proof of concept for, to our knowledge, the first allogeneic CD20xCD22 CAR as an alternative/additional therapy to CD19 CAR T cells with the potential to target B-cell malignancies with heterogeneous levels of CD20 and CD22 expression. Both CD22 and CD20 are well validated and highly expressed targets in B-cell lymphoblastic leukemia and B-NHL (22, 43, 44), that often remain expressed after CD19 relapses (23, 45).

We show that CD20xCD22 CAR T cells exhibit strong cytolytic activity *in vivo* and *in vitro* against tumor cells expressing one or the two antigens. Also, the dual CAR T cells can exert cytotoxic activity and proliferate over time upon exposure to tumors with a single or both antigens. The robust activity observed against primary patient samples with multiple combinations of CD20 and CD22 expression underscores the capability of CD20xCD22 to address heterogenous tumors independently of the levels of the CD19 antigen. While previous publications have reported triple CARs targeting CD19, CD22, and CD20 (45, 46), our dual CAR completely eradicated tumors *in vitro* and *in vivo*. Moreover, our data on primary B-NHL samples indicate that CD20 and CD22 expression are independent, which might increase the chances of treatment success. As we showed, most of the tumor cells obtained from patients previously treated with rituximab continue to express CD20 and were efficiently killed by the CD20xCD22 dual CAR. The observation of CD20 expression in this small set of patients treated with rituximab is in agreement with previous retrospective analyses of CD20 levels in patients with B-NHL relapsing from rituximab treatment (47, 48).

In this study, we also evaluated the antigen-specific activity of the dual CD20xCD22 CAR T cells using a patient-derived xenograft model of MCL, a subtype of B-NHL. With this physiologically relevant model, we observed a significant increase of the overall survival and showed that the dual CAR T cells clear the tumor burden in a dose-dependent manner while releasing cytokines associated with T-cell activity such as IFNγ. Taking all this into account, we hypothesize that allogeneic CD20xCD22 CAR T cells could have the potential to reach a large patient population with heterogeneous CD20 and CD22 levels, while offering an additional therapeutic option for relapses following CD19-directed therapy.

To generate a dual CD20xCD22 CAR, we used a bicistronic lentiviral construct to express both CARs simultaneously in a single cell. Different methodologies have been implemented to date for the production of dual CAR T cells based on either codelivery of two scFVs or CAR molecules with a tandem or a bicistronic construct, or the delivery of two individual constructs (29). Because the generation of a tandem CAR has been associated with a higher complexity on the design to identify an optimal construct (49), we focused on a bicistronic construct. We also confirmed that dual CAR expression in one cell is more efficiently achieved with a bicistronic construct than with two single constructs in this case. Furthermore, the use of a bicistronic

construct can offer several advantages: (i) it can facilitate and reduce costs for large-scale manufacturing for clinical implementation, because only one vector is required; (ii) it has the potential to increase the chances of success for patients expressing low levels of one or the two antigens, and this could benefit heterogenous tumors; and (iii) it potentially strengthens the tumor–CAR T-cell contact (as opposed to having CD20 and CD22 CARs expressed on two separate cells), and thereby enhances the cytotoxic activity in the presence of lower or variable expression levels of the targeted antigens (50). More studies will be needed to decipher the cooperation of these two tumor antigens in increasing synapse strength.

Allogeneic therapies hold the promise to help overcoming some of the challenges associated with manufacturing constrains and T-cell dysfunction identified in some patients in the autologous setting (refs. 51, 52; Supplementary Table S4; refs. 7, 9, 11, 52–59). To respond to this need, different strategies to develop allogeneic cellular therapies have been studied in the last years, including γδT cells, natural killer cells, and gene-edited T cells, which is so far the most advanced approach (7, 60). Supporting this idea, recent studies have demonstrated that using healthy donor T cells to generate CAR T cells can preserve or even improve CAR activity (9, 11, 52). "Off-the-shelf" availability allows the time from treatment decision to therapy infusion to be shortened, which could be decisive in the case of aggressive disease. Moreover, it can bypass challenges associated with potential lower T-cell quality in patients that have undergone several lines of treatment (7). So, the potential benefit of an allogenic product also resides in access to treatment and extends beyond the fact that it is manufactured from healthy T cells. Promising ongoing clinical studies are demonstrating the efficacy and safety (17, 18, 35, 36, 61) of allogeneic therapies and will provide critical information to better understand the potential differences of autologous versus allogeneic CAR T cells in the clinic, as well as to identify potential scenarios where an allogeneic approach would be beneficial. However, because persistence is expected to be lower with allogeneic approaches it is also important to keep in mind that long-term studies remain necessary to evaluate the durability of response and long-term safety of allogeneic approaches.

CD20xCD22 CAR T cells have the potential to be the first allogeneic dual CAR T-cell therapy combining multiple strategies with the aim to provide efficient tumor control: an off-the-shelf approach and dual antigen targeting. TALEN-mediated gene editing of *TRAC* and *CD52* allows the generation of allogeneic CAR T cells readily available at the time of treatment decision, while mitigating the risk of GVHD, facilitating allogeneic engraftment, and increasing the therapeutic window (31). This strategy has been successfully implemented at the manufacturing scale to produce allogeneic CAR T cells and early clinical trials are showing encouraging efficacy and safety data using other targets (13, 16). Using this validated gene-editing scaffold and the abovementioned bicistronic CAR construct, we have now also implemented a large-scale manufacturing process for allogeneic UCART20x22, a non-alloreactive universal dual CAR T-cell product targeting CD20 and CD22, for which the FDA recently cleared an IND and is currently being used in a phase I/IIa clinical study for patients with relapsed/refractory B-cell NHL (clinical trial NatHaLi-01, NCT05607420). Thus, this dual allogeneic CAR T-cell product candidate has the potential to offer a solution for patients whose T cells are dysfunctional and/or for which autologous CAR T-cell manufacturing fails.

In sum, we provide here preclinical proof of concept of an allogeneic dual CAR T cell: CD20xCD22 CAR. This first allogeneic dual CAR T cell targeting two-well validated B-cell antigens has the potential to address some hurdles identified in current CAR T-cell treatment failures, including (i) relapse due to single antigen targeting, tumor heterogeneity, or uneven antigen distribution; (ii) the possibility to use donor "healthy cells" to develop allogeneic CAR T cells, which may increase the potency of the therapy; and (iii) the "off-the-shelf" availability of CAR T cells ready for infusion at the time of treatment decision. Altogether, these data provide a strong rationale supporting allogeneic dual UCART20x22 CAR in a first-in-human clinical trial that has the potential to reach a large patient population.

Authors' Disclosures

B. Aranda-Orgilles reports a patent for WO2022023529A1 pending. I. Chion-Sotinel reports personal fees from Cellectis SA during the conduct of the study; personal fees from Cellectis SA outside the submitted work. P. Erler reports personal fees from Cellectis during the conduct of the study; personal fees from Cellectis outside the submitted work. P. Duchateau is a Cellectis employee. A. Gouble reports personal fees from Cellectis during the conduct of the study; personal fees from Cellectis outside the submitted work. R. Galetto reports personal fees from Cellectis SA during the conduct of the study; personal fees from Cellectis SA outside the submitted work. L. Poirot reports nonfinancial support from Spanish Society of Cell and Gene Therapy (SETGYC) outside the submitted work; in addition, L. Poirot has a patent for WO2022023529 pending. No disclosures were reported by the other authors.

Authors' Contributions

B. Aranda-Orgilles: Conceptualization, formal analysis, supervision, investigation, visualization, methodology, writing–original draft, project administration, writing–review and editing. **I. Chion-Sotinel:** Investigation, visualization, methodology. **J. Skinner:** Investigation, visualization, methodology. **S. Grudman:** Investigation, visualization, methodology. **B. Mumford:** Investigation, visualization, methodology. **C. Dixon:** Investigation, visualization, methodology. **J. Postigo Fernandez:** Visualization, methodology. **P. Erler:** Investigation. **P. Duchateau:** Conceptualization, writing–review and editing. **A. Gouble:** Conceptualization, supervision, methodology, writing–review and editing. **R. Galetto:** Conceptualization, formal analysis, supervision, methodology, writing–review and editing. **L. Poirot:** Conceptualization, supervision, methodology, writing–review and editing.

Acknowledgments

We would like to thank the clinical, translational, process, and analytic development teams at Cellectis for their support thorough this work. We would also like to thank Cellectis publications team for their valuable advice. We are also grateful to Sumin Jo for her generous help with intravenous injections.

The publication costs of this article were defrayed in part by the payment of publication fees. Therefore, and solely to indicate this fact, this article is hereby marked "advertisement" in accordance with 18 USC section 1734.

Note

Supplementary data for this article are available at Cancer Immunology Research Online (http://cancerimmunolres.aacrjournals.org/).

Received November 18, 2022; revised January 25, 2023; accepted May 2, 2023; published first May 31, 2023.

References

1. Thandra KC, Barsouk A, Saginala K, Padala SA, Barsouk A, Rawla P. Epidemiology of non-Hodgkin's lymphoma. Med Sci 2021;9:5.
2. Sung H, Ferlay J, Siegel RL, Laversanne M, Soerjomataram I, Jemal A, et al. Global cancer statistics 2020: GLOBOCAN estimates of incidence and

mortality worldwide for 36 cancers in 185 countries. CA Cancer J Clin 2021; 71:209–49.
3. Davila ML, Brentjens RJ. CD19-targeted CAR T cells as novel cancer immunotherapy for relapsed or refractory B-cell acute lymphoblastic leukemia. Clin Adv Hematol Oncol 2016;14:802–8.
4. Spiegel JY, Patel S, Muffly L, Hossain NM, Oak J, Baird JH, et al. CAR T cells with dual targeting of CD19 and CD22 in adult patients with recurrent or refractory B cell malignancies: a phase 1 trial. Nat Med 2021;27:1419–31.
5. Wang L. Clinical determinants of relapse following CAR-T therapy for hematologic malignancies: coupling active strategies to overcome therapeutic limitations. Curr Res Transl Med 2022;70:103320.
6. Amini L, Silbert SK, Maude SL, Nastoupil LJ, Ramos CA, Brentjens RJ, et al. Preparing for CAR T cell therapy: patient selection, bridging therapies and lymphodepletion. Nat Rev Clin Oncol 2022;19:342–55.
7. Depil S, Duchateau P, Grupp SA, Mufti G, Poirot L. 'Off-the-shelf' allogeneic CAR T cells: development and challenges. Nat Rev Drug Discov 2020;19:185–99.
8. Lundh S, Maji S, Melenhorst JJ. Next-generation CAR T cells to overcome current drawbacks. Int J Hematol 2021;114:532–43.
9. Metelo AM, Jozwik A, Luong LA, Dominey-foy D, Attwood C, Inam S, et al. Allogeneic anti-BCMA CAR T cells are superior to multiple myeloma-derived CAR T cells in preclinical studies and may be combined with gamma secretase inhibitors. Cancer Res Commun 2022;2:158–71.
10. Hoffmann JM, Schubert ML, Wang L, Hückelhoven A, Sellner L, Stock S, et al. Differences in expansion potential of naive chimeric antigen receptor T cells from healthy donors and untreated chronic lymphocytic leukemia patients. Front Immunol 2018;8:1956.
11. Graham CE, Jozwik A, Quartey-Papafio R, Ioannou N, Metelo AM, Scala C, et al. Gene-edited healthy donor CAR T cells show superior anti-tumour activity compared to CAR T cells derived from patients with lymphoma in an *in vivo* model of high-grade lymphoma. Leukemia 2021;35:3581–4.
12. Martínez Bedoya D, Dutoit V, Migliorini D. Allogeneic CAR T cells: an alternative to overcome challenges of CAR T cell therapy in glioblastoma. Front Immunol 2021;12:640082.
13. Neelapu SS, Nath R, Munoz J, Tees M, Miklos DB, Frank MJ, et al. ALPHA study: ALLO-501 produced deep and durable responses in patients with relapsed/refractory non-Hodgkin's lymphoma comparable to autologous CAR T. Blood 2021;138:3878.
14. Sallman DA, DeAngelo DJ, Pemmaraju N, Dinner S, Gill S, Olin RL, et al. Ameli-01: a phase i trial of UCART123v1.2, an anti-CD123 allogeneic CAR-T cell product, in adult patients with relapsed or refractory (R/R) CD123+ acute myeloid leukemia (AML). Blood 2022;140:2371–3.
15. Lekakis LJ, Locke FL, Tees M, Neelapu SS, Malik SA, Hamadani M, et al. ALPHA2 study: ALLO-501A allogeneic CAR T in LBCL, updated results continue to show encouraging safety and efficacy with consolidation dosing. Blood 2021;138:649.
16. Benjamin R, Jain N, Maus MV, Boissel N, Graham C, Jozwik A, et al. UCART19, a first-in-class allogeneic anti-CD19 chimeric antigen receptor T-cell therapy for adults with relapsed or refractory B-cell acute lymphoblastic leukaemia (CALM): a phase 1, dose-escalation trial. Lancet Haematol 2022;9:e833–43.
17. Jain N, Roboz GJ, Konopleva M, Liu H, Schiller GJ, Jabbour EJ, et al. Preliminary results from the flu/cy/alemtuzumab arm of the phase I BALLI-01 trial of UCART22, an anti-CD22 allogeneic CAR-T cell product, in adult patients with relapsed or refractory (R/R) CD22+ B-cell acute lymphoblastic leukemia (B-ALL). Blood 2021;138:1746.
18. McGuirk J, Bachier CR, Bishop MR, Ho PJ, Murthy HS, Dickinson MJ, et al. A phase 1 dose escalation and cohort expansion study of the safety and efficacy of allogeneic CRISPR-Cas9–engineered T cells (CTX110) in patients (Pts) with relapsed or refractory (R/R) B-cell malignancies (CARBON). J Clin Oncol 39: 15s, 2021 (suppl; abstr TPS7570).
19. Shah BD, Jacobson C, Solomon SR, Jain N, Johnson MC, Vainorius M, et al. Allogeneic CAR-T PBCAR0191 with intensified lymphodepletion is highly active in patients with relapsed/refractory B-cell malignancies. Blood 2021; 138:302.
20. Neelapu SS, Locke FL, Bartlett NL, Lekakis LJ, Miklos DB, Jacobson CA, et al. Axicabtagene ciloleucel CAR T-cell therapy in refractory large B-cell lymphoma. N Engl J Med 2017;377:2531–44.
21. Xie B, Li Z, Zhou J, Wang W. Current status and perspectives of dual-targeting chimeric antigen receptor T-cell therapy for the treatment of hematological malignancies. Cancers 2022;14:3230.
22. Köksal H, Dillard P, Josefsson SE, Maggadottir SM, Pollmann S, Fane A, et al. Preclinical development of CD37CAR T-cell therapy for treatment of B-cell lymphoma. Blood Adv 2019;3:1230–43.
23. Neelapu SS, Rossi JM, Jacobson CA, Locke FL, Miklos DB, Reagan PM, et al. CD19-loss with preservation of other B cell lineage features in patients with large B cell lymphoma who relapsed post-axi-cel. Blood 2019; 134:203.
24. Haso W, Lee DW, Shah NN, Stetler-Stevenson M, Yuan CM, Pastan IH, et al. Anti-CD22-chimeric antigen receptors targeting B-cell precursor acute lymphoblastic leukemia. Blood 2013;121:1165–74.
25. Teeling JL, French RR, Cragg MS, Van Den Brakel J, Pluyter M, Huang H, et al. Characterization of new human CD20 monoclonal antibodies with potent cytolytic activity against non-Hodgkin lymphomas. Blood 2004;104:1793–800.
26. Yang M, Tkach D, Boyne A, Kazancioglu S, Duclert A, Poirot L, et al. Optimized two-step electroporation process to achieve efficient nonviral-mediated gene insertion into primary T cells. FEBS Open Bio 2022;12:38–50.
27. Valton J, Guyot V, Boldajipour B, Sommer C, Pertel T, Juillerat A, et al. A versatile safeguard for chimeric antigen receptor T-cell immunotherapies. Sci Rep 2018;8:8972.
28. Sachdeva M, Busser BW, Temburni S, Jahangiri B, Gautron AS, Maréchal A, et al. Repurposing endogenous immune pathways to tailor and control chimeric antigen receptor T cell functionality. Nat Commun 2019;10:5100.
29. Majzner RG, Mackall CL. Tumor antigen escape from car t-cell therapy. Cancer Discov 2018;8:1219–26.
30. Long AH, Haso WM, Shern JF, Wanhainen KM, Murgai M, Ingaramo M, et al. 4-1BB costimulation ameliorates T cell exhaustion induced by tonic signaling of chimeric antigen receptors. Nat Med 2015;21:581–90.
31. Sugita M, Galetto R, Zong H, Ewing-Crystal N, Trujillo-Alonso V, Mencia-Trinchant N, et al. Allogeneic TCRαβ deficient CAR T-cells targeting CD123 in acute myeloid leukemia. Nat Commun 2022;13:2227.
32. Ho JY, Wang L, Liu Y, Ba M, Yang J, Zhang X, et al. Promoter usage regulating the surface density of CAR molecules may modulate the kinetics of CAR-T cells *in vivo*. Mol Ther Methods Clin Dev 2021;21:237–46.
33. Philip LPB, Schiffer-Mannioui C, Le Clerre D, Chion-Sotinel I, Derniame S, Potrel P, et al. Multiplex genome-edited T-cell manufacturing platform for "off-the-shelf" adoptive T-cell immunotherapies. Cancer Res 2015;75:3853–64.
34. Benjamin R, Graham C, Yallop D, Jozwik A, Ciocarlie O, Jain N, et al. Preliminary data on safety, cellular kinetics and anti-leukemic activity of UCART19, an allogeneic anti-CD19 CAR T-cell product, in a pool of adult and pediatric patients with high-risk CD19+ relapsed/refractory B-cell acute lymphoblastic leukemia. Blood 2018;132:896.
35. Mailankody S, Liedtke M, Sidana S, Matous JV, Chhabra S, Oluwole OO, et al. Universal updated phase 1 data validates the feasibility of allogeneic anti-BCMA ALLO-715 therapy for relapsed/refractory multiple myeloma. Blood 2021;138: 651.
36. Benjamin R, Graham C, Yallop D, Jozwik A, Mirci-Danicar OC, Lucchini G, et al. Genome-edited, donor-derived allogeneic anti-CD19 chimeric antigen receptor T cells in paediatric and adult B-cell acute lymphoblastic leukaemia: results of two phase 1 studies. Lancet 2020;396:1885–94.
37. Qin H, Ramakrishna S, Nguyen S, Fountaine TJ, Ponduri A, Stetler-Stevenson M, et al. Preclinical development of bivalent chimeric antigen receptors targeting both CD19 and CD22. Mol Ther Oncolytics 2018;11:127–37.
38. Shah NN, Highfill SL, Shalabi H, Yates B, Jin J, Wolters PL, et al. CD4/CD8 T-cell selection affects chimeric antigen receptor (CAR) T-cell potency and toxicity: updated results from a phase I anti-CD22 CAR T-cell trial. J Clin Oncol 2020;38: 1938–50.
39. Park JH, Rivière I, Gonen M, Wang X, Sénéchal B, Curran KJ, et al. Long-term follow-up of CD19 CAR therapy in acute lymphoblastic leukemia. N Engl J Med 2018;378:449–59.
40. Zhao J, Song Y, Liu D. Clinical trials of dual-target CAR T cells, donor-derived CAR T cells, and universal CAR T cells for acute lymphoid leukemia. J Hematol Oncol 2019;12:17.
41. Shalabi H, Qin H, Su A, Yates B, Wolters PL, Steinberg SM, et al. CD19/22 CAR T-cells in children and young adults with B-ALL: phase I results and development of a novel bicistronic CAR. Blood 2022;140:451–63.
42. Fernández de Larrea C, Staehr M, Lopez AV, Ng KY, Chen Y, Godfrey WD, et al. Defining an optimal dual-targeted CAR T-cell therapy approach simultaneously targeting BCMA and GPRC5D to prevent BCMA escape–driven relapse in multiple myeloma. Blood Cancer Discov 2020;1:146–54.

43. Lanza F, Maffini E, Rondoni M, Massari E, Faini AC, Malavasi F. CD22 expression in B-cell acute lymphoblastic leukemia: biological significance and implications for inotuzumab therapy in adults. Cancers 2020;12:303.
44. Kosmas C, Stamatopoulos K, Stavroyianni N, Tsavaris N, Papadaki T. Anti-CD20-based therapy of B cell lymphoma: state of the art. Leukemia 2002;16: 2004–15.
45. Fousek K, Watanabe J, Joseph SK, George A, An X, Byrd TT, et al. CAR T-cells that target acute B-lineage leukemia irrespective of CD19 expression. Leukemia 2021;35:75–89.
46. Schneider D, Xiong Y, Wu D, Hu P, Alabanza L, Steimle B, et al. Trispecific CD19-CD20-CD22-targeting duoCAR-T cells eliminate antigen-heterogeneous B cell tumors in preclinical models. Sci Transl Med 2021;13:eabc6401.
47. Rasheed AA, Samad A, Raheem A, Hirani SI, Shabbir- Moosajee M. Cd20 expression and effects on outcome of relapsed/refractory diffuse large B cell lymphoma after treatment with rituximab. Asian Pacific J Cancer Prev 2018;19: 331–5.
48. Marshalek JP, Dragan M, Tomassetti S, LaBarbera K, Amaya A. CD20 and CD19 expression loss in relapsed or refractory B-cell non-Hodgkin lymphoma: a retrospective cohort. J Clin Oncol 40:16s, 2022 (suppl; abstr e19537).
49. Tong C, Zhang Y, Liu Y, Ji X, Zhang W, Guo Y, et al. Optimized tandem CD19/CD20 CAR-engineered T cells in refractory/relapsed B-cell lymphoma. Blood 2020;136:1632–44.
50. Ruella M, Barrett DM, Kenderian SS, Shestova O, Hofmann TJ, Perazzelli J, et al. Dual CD19 and CD123 targeting prevents antigen-loss relapses after CD19-directed immunotherapies. J Clin Invest 2016;126:3814–26.
51. Mehta PH, Fiorenza S, Koldej RM, Jaworowski A, Ritchie DS, Quinn KM. T cell fitness and autologous CAR T cell therapy in haematologic malignancy. Front Immunol 2021;12:780442.
52. Fraietta JA, Lacey SF, Orlando EJ, Pruteanu-Malinici I, Gohil M, Lundh S, et al. Determinants of response and resistance to CD19 chimeric antigen receptor (CAR) T cell therapy of chronic lymphocytic leukemia. Nat Med 2018;24:563–71.
53. Caldwell KJ, Gottschalk S, Talleur AC. Allogeneic CAR cell therapy—more than a pipe dream. Front Immunol 2021;11:618427.
54. Shah NN, Fry TJ. Mechanisms of resistance to CAR T cell therapy. Nat Rev Clin Oncol 2019;16:372–85.
55. Melenhorst JJ, Chen GM, Wang M, Porter DL, Chen C, Collins MKA, et al. Decade-long leukaemia remissions with persistence of CD4+ CAR T cells. Nature 2022;602:503–9.
56. Bethge WA, Martus P, Schmitt M, Holtick U, Subklewe M, von Tresckow B, et al. GLA/DRST real-world outcome analysis of CAR-T cell therapies for large B-cell lymphoma in Germany. Blood 2022;140:349–58.
57. Bachy E, Le Gouill S, Di Blasi R, Sesques P, Manson G, Cartron G, et al. A real-world comparison of tisagenlecleucel and axicabtagene ciloleucel CAR T cells in relapsed or refractory diffuse large B cell lymphoma. Nat Med 2022; 28:2145–54.
58. Graham C, Jozwik A, Pepper A, Benjamin R. Allogeneic car-t cells: more than ease of access? Cells 2018;7:155.
59. Pasquini MC, Hu Z-H, Curran K, Laetsch T, Locke F, Rouce R, et al. Real-world evidence of tisagenlecleucel for pediatric acute lymphoblastic leukemia and non-Hodgkin lymphoma. Blood Adv 2020;4:5414–24.
60. Patel S, Burga RA, Powell AB, Chorvinsky EA, Hoq N, McCormack SE, et al. Beyond CAR T cells: other cell-based immunotherapeutic strategies against cancer. Front Oncol 2019;9:196.
61. Qasim W, Zhan H, Samarasinghe S, Adams S, Amrolia P, Stafford S, et al. Molecular remission of infant B-ALL after infusion of universal TALEN gene-edited CAR T cells. Sci Transl Med 2017;9:eaaj2013.